Available online at www.sciencedirect.com

ScienceDirect

Procedia Manufacturing 3 (2015) 3759 – 3766

Procedia MANUFACTURING

6th International Conference on Applied Human Factors and Ergonomics (AHFE 2015) and the Affiliated Conferences, AHFE 2015

A composite method for human foot structural modeling

KaiWei Zhao, Ameersing Luximon*, Balasankar Ganesan, CheeKooi Chan

Institute of Textiles and Clothing, The Hong Kong Polytechnic University, Hung Hom, Kowloon, Hong Kong

Abstract

A novel method including range-sensing scanning with texture and foot anatomical structure morphing basing on OpenSim is proposed. Palpation of important anatomical landmarks on foot surface was conducted by a physical therapist, and a range-sensing device, Microsoft Kinect sensor, was adopted for the 3D textured model acquisition. 3D coordinate data of the landmarks were measured and harnessed in OpenSim for subject-specific skeletal scaling based on a generic foot musculoskeletal model. The muscle attachment point coordinates derived from an anatomy database basing on sampling from East Asia people were used for muscle modelling. Then the 3D textured foot surface was registered with the morphed anatomical structures so that an integrated foot model was generated. The surface landmark locations were then compared with the corresponding internal bony sites and the errors were calculated to evaluate the accuracy and validity of this method. The potential error sources such as soft tissue thickness and scaling error were also mentioned and discussed. This technique is useful to create individual anatomically accurate human digital models for product design and development.

Keywords: Musculoskeletal modeling; Subject-specific morph; Range-sensing scan; Integrated foot model

1. Introduction

The uses of the digital anatomical foot model are fairly broad: pathology mechanics [1], plantar pressure [2], plantar fasciitis [3] and surgical interventions [4]. In the fields of orthotic design [5] and shoe design [6], there are also successful application instances. In order to get accurate details of anatomical structure inside the human body, Computerized Tomography (CT) and Magnetic Resonance Imaging (MRI) have been used.

* Corresponding author. Tel.: 852 2766 6449; fax: 852 2773 1432.
E-mail address: tcshyam@polyu.edu.hk

doi:10.1016/j.promfg.2015.07.821

CT scans are good at bone density and geometry detection while MRI is highly applicable to soft tissue imaging. Although with different imaging principles, the two approaches share some similar pros and cons. The output data from both MRI and CT are segmented into slices thereby facilitating for the geometrical reconstruction. With weak contrast between soft tissues and bone, MRI manifests one of its drawbacks. In this regard, CT does better, but the exposure to radiation leaves this method a fatal limitation in terms of the convenience of research. What they share are the high cost and serious inconvenience due to their matched high-end equipment [7], which makes both methods time consuming and impractical for individual model customization use.

Taking the features of CT and MRI into consideration, researchers harness a standard or reference model (developed from MRI or CT) that can be generated basing on real human anatomy data beforehand and then morph it to fit a specific subject according to surface geometry and anatomical landmarks of the specific body part [8]. Using this method, the subject-specific model can be efficiently and accurately acquired although it is just a predicted result. When focusing on foot surface shape acquisition, which may include even the color and texture of the scanned foot, the palpation procedure is commonly arranged corresponding to the important bone and joint landmarks on the foot skin and thereby colored stickers can be used [9]. Compared to medical imaging technology, the doctor and technician prefer to use this traditional method for anatomy structure evaluation, since even today it still has considerable application value as a non-invasive and highly-efficient anthropometry method. Besides, this approach also has an advantage that anatomical landmarks can be assigned beforehand and recognized after scanning both manually and automatically through programming [10]. Essentially, musculoskeletal foot model should be contained as a significant component in this approach. Several researchers have already developed some anatomical models with the aim of anthropometry or muscle function estimation [11,12,13,14,15]. Some of them directly harnessed the existing model provided by biomechanical analysis software such as Anybody and LifeMOD, which gave rise to unpredictable errors due to non-specificity of the musculoskeletal structure. Others developed the lower limb models themselves but based on the anatomy database statistically derived from Caucasians [16]. In view of this, we adopted a new lower limb anatomy database developed by Shan (2003) [17] specially based on people of Asian race from East Asia, thus the muscle attachment locations will be more accurate for future analysis.

In terms of the 3D scanning method for foot shape geometry acquisition, one of the methods is to use foot laser scanner. There are now various foot scanning systems available, but they are expensive, e.g. the Scan 3D foot scanner cost around US$51600. Optical scanner (e.g. a laser scanner) is a non-invasive scanning equipment with advantages of high accuracy (up to 0.1mm [18]) compared to traditional method, such as casting. However, the more accurate it is, the higher it costs, and the worse portability the device will be. This is so inconvenient and impractical in certain cases when people need a solution with high efficiency, portability while not with requirement of such a precision. Range sensing equipment is recently developing fast. This approach is on the basis of light coding, projecting a known infrared pattern onto the object and depth data is hence determined based on deforming information of infrared pattern. They cost much less accompanied by owning better portability and efficiency. A most representative one is Microsoft Kinect (Microsoft LTD.), which was adopted to capture the foot geometry data with landmarks through its color information in this study.

In this study, we proposed a composite method to develop a morphed three segment foot anatomical structure based on range sensing scanning including surface landmarks, a generic musculoskeletal model [19] and the aforementioned anthropometric anatomy database. OpenSim (open-source software from Stanford University) is also used as the morphing tool in order that the basic correlation between the skeleton and muscles / ligaments is preset properly. The landmark location validation was also conducted after registration of the foot surface and the internal anatomical structure.

2. Methods

2.1. Foot surface data acquisition

Five female subjects (between 20~25 year old) were invited to the foot scan experiment using Kinect scanning system. Besides Microsoft Kinect Sensor, the setup also includes a high performance Laptop (MSI LTD.) and Artec Studio 9 (Artec LTD.) for real-time data processing and visualization [20]. The experiment was started with the subject standing normally on the ground. The projector lens on Kinect sensor should be kept facing directly to the

object while moving around so that Artec Studio would keep tracking the scene within its field of vision. During the whole procedure the operator should move the Kinect sensor smoothly. Frame data is in real time calculated and displayed. After scanning, Artec Studio would conduct post-processing including global registration and texture mapping basing on all the frame data. The generated 3D textured foot model is demonstrated in Fig. 1.

Meshlab software is adopted for mesh data process such as further noise removal. In Geomagic Studio (Geomagic LTD.), coordinates of the landmarks (black) on the foot surface can be extracted and utilized in the anatomical morphing as tool landmarks. Accuracy check of Kinect scanning system utilized in this study was also carried out [21]. In terms of foot scan, we are able to achieve an average precision of around 1.5mm.

2.2. Subject-specific morphing of musculoskeletal structures

The generic lower extremity model (LowerLimbModel2010_2LegsHATv2.1) in OpenSim model library was used for foot model morphing (Fig. 2). The red dots are the landmarks as the scaling tools. Their locations (3D coordinates) corresponding to the homologous ones marked on the subjects' feet were used to morph the generic model into subject-specific ones.

At first, the anatomical landmarks (pink balls in OpenSim interface) are matched one-to-one with the black markers we put on the subjects' foot surface. Then the dimension between two bony landmarks, taking metatarsal-phalangeal joint and inter-phalangeal joint as an example, can be measured on the 3D model within MeshLab or Geomagic Studio. The corresponding input area of this dimension in OpenSim can now be filled in with the value we obtained. Alternative and more frequently used parameters are the coordinates of the markers which require consistent reference frame fixed on the skeletal segment. The scaling ratio, as a result, will also be revealed. In this study, we adopted uniform scaling method, i.e. scale the generic segments (Fig. 3) uniformly according to the ratio (Fig. 4).

Fig. 1. 3D textured foot model from Kinect scanning system.

Fig. 2. Foot model in OpenSim (white: skeleton; red: muscles).

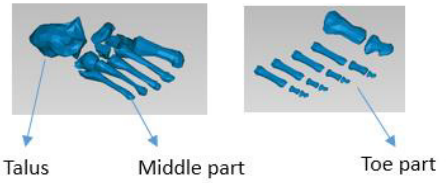

Fig. 3. Toe segment: includes all phalanx distalis, phalanx media and phalanx proximalis; middle segment: includes all the metatarsal bones; the talus.

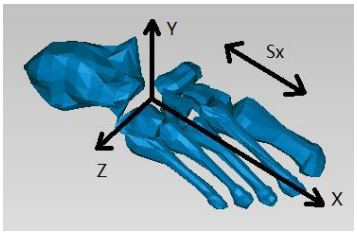

$$\begin{bmatrix} S_x & 0 & 0 \\ 0 & S_y & 0 \\ 0 & 0 & S_z \end{bmatrix}$$

Fig. 4. Representation of morphing and the transforming matrix ($Sx = Sy = Sz$).

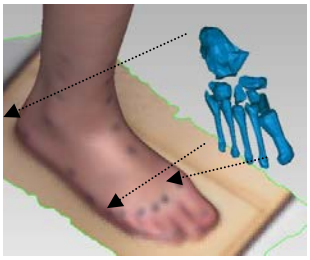

Fig. 5. Homologous landmarks matching.

The Registration step based on matching of coloured markers on the scanned surface and bony landmarks on the morphed skeleton are carried out when the morphing is finished. As illustrated in Fig. 5, the homologous landmarks are attached together based on least-squares criterion:

$$F = \min \sum_{i=1}^{n} Dist^2(P_{Mi}, P_{Ri}) \tag{1}$$

where $Dist\ (P_{Mi}\ ,\ P_{Ri})$ denotes the distance between one pair of corresponding markers from the generic and morphed model, respectively. F is the cost function that should be minimized. The morphed rigid point set (with constant distances between each other) were located and oriented through rigid transformation [22]. The whole flow chart of the skeleton morphing work is shown in Fig. 6.

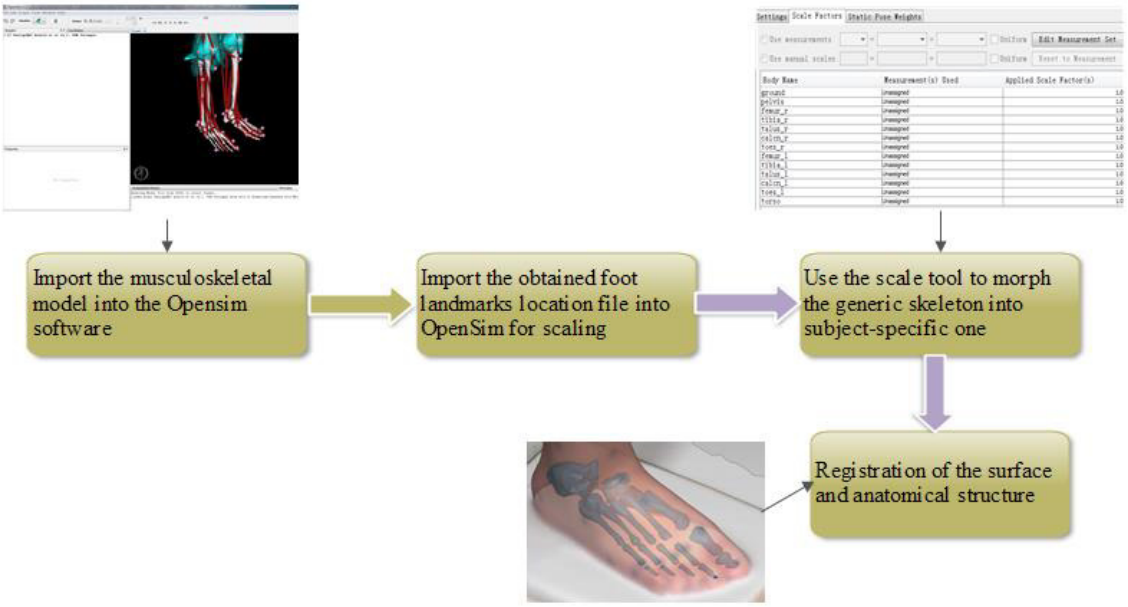

Fig. 6. The flow chart of morphing a generic model into a subject-specific one, also with the registration step (Lochner et al., 2014) applied in Geomagic Studio to generate the integrated foot model.

Muscle and ligament are also of great significance in foot anatomical structures. They can also be edited according to the database created by Shan (2003) [17] basing on our morphed skeleton. Tab.1 shows the statistical coordinates of the muscles and ligaments attachment locations of foot of Asians from East Asia. The average muscle attachment locations were calculated through sampling from the cadavers (also with regression equations depending on multiple bony morphological parameters). In this paper, we chose from the female set of the database and use the average locations in the musculoskeletal model. Accordingly the attachment points were edited in OpenSim and illustrated in Fig.7.

Table 1. The average muscle attachment locations [17].

Muscle attachment points	X (mm)	Y (mm)	Z (mm)	Reference frame
Tibialis Anterior origin	2.08 ±0.07	1.15 ±0.04	–2.07 ±1.05	Tibia
Tibialis Anterior insertion	6.82 ±1.17	–3.52 ±0.08	–1.47 ±0.12	Foot
Extensor Digitorum Longus origin	2.28 ±0.33	0.96 ±0.70	1.14 ±0.56	Tibia
Extensor Digitorum Longus insertion	10.80 ±0.45	–4.69 ±0.68	2.57 ±0.11	Foot
Extensor Hallucis Longus insertion	12.76 ±0.73	–3.78 ±1.15	–1.43 ±0.08	Foot
Tibialis Posterior origin	1.17 ±0.25	0.26 ±0.52	–2.46 ±0.13	Tibia
Tibialis Posterior insertion	3.37 ±2.14	–3.19 ±0.22	–1.45 ±0.08	Foot
Flexor Digitorum Longus origin	–2.07 ±0.52	0.52 ±1.07	–1.16 ±0.65	Tibia
Flexor Digitorum Longus insertion	0.54 ±0.02	–2.98 ±0.13	–0.53 ±0.07	Foot
Flexor Hallucis Longus insertion	0.54 ±0.02	–2.98 ±0.13	–0.53 ±0.07	Foot
Peroneus Longus origin	–1.87 ±0.79	–1.07 ±0.48	1.99 ±0.11	Tibia
Peroneus Longus insertion	4.51 ±0.21	–5.90 ±0.32	4.02 ±0.81	Foot
Peroneus Brevis origin	–1.87 ±0.79	–1.07 ±0.48	1.99 ±0.11	Tibia
Peroneus Brevis insertion	4.51 ±0.21	–5.90 ±0.32	4.02 ±0.81	Foot
Peroneus Tertius origin	1.72 ±0.14	0.64 ±0.15	2.40 ±0.07	Tibia
Peroneus Tertius insertion	5.19 ±0.01	–4.72 ±0.32	4.34 ±0.11	Foot

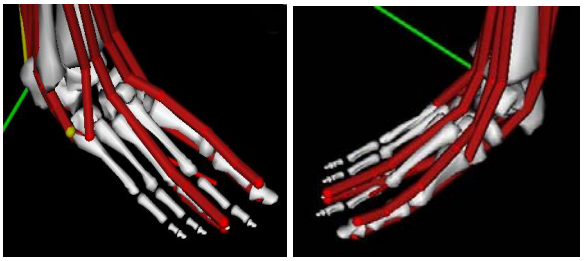

Fig. 7. Muscles modeled via attachment points on the skeleton.

3. Results

The five registered integrated foot models are shown in Fig.8. The surface landmark coordinates and their corresponding bony positions on the skeleton model are all measured in Geomagic Studio in order that they can be compared (Fig.9). Tab.2 reveals the measurement results (the skin thickness has been neglected).

Table 2. Deviations between surface landmarks and bony sites (6 bony landmarks were sampled).

The measured positions	Deviation (mm)					
	Sub 1	Sub 2	Sub 3	Sub 4	Sub 5	Average
First MTP joint	3.232	2.661	4.120	2.225	4.027	3.253
Tip of the second toe	2.211	3.359	3.378	3.078	3.559	3.117
Tip of the 3 toe	2.583	1.438	2.553	3.768	1.786	2.426
Tip of the 4th toe	3.353	3.245	2.577	2.294	3.798	3.053
Tip of the 5th toe	3.067	2.545	3.071	2.885	1.095	2.533
Lateral side of the 5th metatarsal head or 5th metatarsal joint	1.254	2.879	1.421	1.332	2.021	1.781

Fig. 8. The skeleton-surface registered foot models basing on bony landmarks.

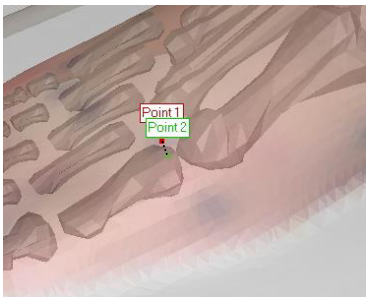

Fig. 9. Measurement of two corresponding points between surface landmark and bony position (dashed line).

4. Conclusion and discussion

We adopted six typical bony landmarks for the results demonstration. What is worth to mention is the foot skin thickness is neglected in this study. According to Shuster et al. (1975) [23], the skin thickness of female is 1.2mm on average. If the results are calibrated with this value, a 1~2mm error, which is close to the precision of Kinect scanning system [20], will be revealed in the results. Admittedly, there are other error sources such as palpation inaccuracy and scaling error, which will be further explored basing on larger sample size and advanced medical equipment, e.g. pulse ultrasound device which can also utilized for measuring foot upper skin thickness. There are similar work done by other researchers harnessing MRI technology together with image segmentation and 3D reconstruction [24]. Although higher accuracy and musculoskeletal customization are obtained, the time and labour consuming work and unwillingness of subjects to participate in characterize the conventional method by poor convenience, operability, accessibility and more significant, high cost. The method proposed in this paper can considerably avoid the drawbacks aforementioned and also produces practical precision for footwear applications. However, this study still needs further research due to lack of high-end medical devices for soft tissue structure detection and validation, such as validation of foot muscle attachment locations. The morphing approach, especially, requires modification focusing on multiple degrees of freedom (DOF) affine transformation. Besides, since there are little inter-individual variation at the interface of two bones, the joint structures in the generic reference model (derived from either cadaver anatomy database or MRI data statistically) will be kept fixed during the morphing procedure with only the bones sharing this joint scaled. The method proposed contributes to musculoskeletal integrated modeling of female foot. The results demonstrated decent average error after skeletal morphing and registration between the textured foot surface and the internal anatomical structures.

Acknowledgements

The authors thank the Hong Kong polytechnic University and the Hong Kong Research Grant Council for their support. This study was supported by funds from the research grant council “RGC Ref. No. 546412”.

References

[1] Cheung, J. T.-M., Zhang, M., An, K.-N. (2006). Effect of Achilles tendon loading on plantar fascia tension in the standing foot. Clinical Biomechanics, 21(2), 194-203.

[2] Actis, R. L., Ventura, L. B., Smith, K. E., Commean, P. K., Lott, D. J., Pilgram, T. K., Mueller, M. J. (2006). Numerical simulation of the plantar pressure distribution in the diabetic foot during the push-off stance. Medical and biological engineering and computing, 44(8), 653-663.

[3] Cheng, H.-Y. K., Lin, C.-L., Wang, H.-W., Chou, S.-W. (2008). Finite element analysis of plantar fascia under stretch-the relative contribution of windlass mechanism and Achilles tendon force. Journal of Biomechanics, 41(9), 1937-1944.

[4] A García-González, A., Bayod, J., Prados-Frutos, J. C., Losa-Iglesias, M., Jules, K. T., de Bengoa-Vallejo, R. B., Doblaré, M. (2009). Finite-element simulation of flexor digitorum longus or flexor digitorum brevis tendon transfer for the treatment of claw toe deformity. Journal of Biomechanics, 42(11), 1697-1704.
[5] Cheung, J. T.-M., Zhang, M. (2008). Parametric design of pressure-relieving foot orthosis using statistics-based finite element method. Medical engineering & physics, 30(3), 269-277.
[6] Even-Tzur, N., Weisz, E., Hirsch-Falk, Y., Gefen, A. (2006). Role of EVA viscoelastic properties in the protective performance of a sport shoe: computational studies. Bio-medical materials and engineering, 16(5), 289-299.
[7] Lochner, S. J., Huissoon, J. P., Bedi, S. S. (2014). Development of a patient-specific anatomical foot model from structured light scan data. Computer methods in biomechanics and biomedical engineering, 17(11), 1198-1205.
[8] Sigal, I. A., Yang, H., Roberts, M. D., Downs, J. C. (2010). Morphing methods to parameterize specimen-specific finite element model geometries. Journal of Biomechanics, 43(2), 254-262.
[9] MacWilliams, B. A., Cowley, M., Nicholson, D. E. (2003). Foot kinematics and kinetics during adolescent gait. Gait & posture, 17(3), 214-224.
[10] Baek, S.-Y., Wang, J.-H., Song, I., Lee, K., Lee, J., Koo, S. (2013). Automated bone landmarks prediction on the femur using anatomical deformation technique. Computer-Aided Design, 45(2), 505-510.
[11] Damsgaard, M., Rasmussen, J., Christensen, S. T., Surma, E., de Zee, M. (2006). Analysis of musculoskeletal systems in the AnyBody Modeling System. Simulation Modelling Practice and Theory, 14(8), 1100-1111.
[12] Hoy, M. G., Zajac, F. E., Gordon, M. E. (1990). A Musculoskeletal Model of the Human Lower-Extremity - the Effect of Muscle, Tendon, and Moment Arm on the Moment Angle Relationship of Musculotendon Actuators at the Hip, Knee, and Ankle. Journal of biomechanics, 23(2), 157-169.
[13] Modenese, L., Gopalakrishnan, A., Phillips, A. T. (2013). Application of a falsification strategy to a musculoskeletal model of the lower limb and accuracy of the predicted hip contact force vector. J Biomech, 46(6), 1193-1200.
[14] Saraswat, P., Andersen, M. S., Macwilliams, B. A. (2010). A musculoskeletal foot model for clinical gait analysis. J Biomech, 43(9), 1645-1652.
[15] Sartori, M., Reggiani, M., Lloyd, D. G., Pagello, E. (2010). An EMG-driven Musculoskeletal Model of the Human Lower Limb for the Estimation of Muscle Forces and Moments at the Hip, Knee and Ankle Joints in vivo. Paper presented at the Proc. of Int. Conf. on Simulation, Modeling and Programming for Autonomous Robots.
[16] Brand, R. A., Crowninshield, R. D., Wittstock, C. E., Pedersen, D. R., Clark, C. R., van Krieken, F. M. (1982). A model of lower extremity muscular anatomy. J Biomech Eng, 104(4), 304-310.
[17] Shan, D.-m. (2003). Study on the muscular function model and its application of human lower extremity. SPORTS SCIENCE RESEARCH, 24(4), 16-20.
[18] Bradley, C., Currie, B. (2005). Advances in the field of reverse engineering. Computer-Aided Design and Applications, 2(5), 697-706.
[19] Delp, S. L., Loan, J. P., Hoy, M. G., Zajac, F. E., Topp, E. L., Rosen, J. M. (1990). An interactive graphics-based model of the lower extremity to study orthopaedic surgical procedures. IEEE Trans Biomed Eng, 37(8), 757-767.
[20] Zhao, K., Luximon, A., Balasankar, G., Chan, C. (2014). A New Representational Method of Human Foot Anatomical Landmark and its Application in Foot Posture Data Acquisition. Advances in Applied Digital Human Modeling, 4, 79.
[21] Zhao, K., Luximon, A, Chan, C. (2015). Low cost 3D foot scan with Kinect. Int. J. of the Digital Human (accepted and revised).
[22] Sharp, G. C., Lee, S. W., Wehe, D. K. (2002). ICP registration using invariant features. Ieee Transactions on Pattern Analysis and Machine Intelligence, 24(1), 90-102.
[23] Shuster, S., Black, M. M., McVitie, E. (1975). The influence of age and sex on skin thickness, skin collagen and density. Br J Dermatol, 93(6), 639-643.
[24] Schmid, J., Sandholm, A., Chung, F., Thalmann, D., Delingette, H., Magnenat-Thalmann, N. (2009). Musculoskeletal simulation model generation from MRI data sets and motion capture data Recent advances in the 3D Physiological Human (pp. 3-19): Springer.